Available online at www.sciencedirect.com
ScienceDirect
Journal of Magnetic Resonance 187 (2007) 306–313
JMR Journal of Magnetic Resonance
www.elsevier.com/locate/jmr

Experimental implementation of a three qubit quantum game with corrupt source using nuclear magnetic resonance quantum information processor

Avik Mitra [a,*], K. Sivapriya [b], Anil Kumar [a]

[a] NMR Quantum Computation and Quantum Information Group, Department of Physics and NMR Research Centre, Indian Institute of Science, Bangalore 560012, India
[b] Department of Organic Chemistry, Indian Institute of science, Bangalore 560012, India

Received 1 February 2007; revised 16 May 2007
Available online 2 June 2007

Abstract

In a three player quantum 'Dilemma' game each player takes independent decisions to maximize his/her individual gain. The optimal strategy in the quantum version of this game has a higher payoff compared to its classical counterpart. However, this advantage is lost if the initial qubits provided to the players are from a noisy source. We have experimentally implemented the three player quantum version of the 'Dilemma' game as described by Johnson, [N.F. Johnson, Phys. Rev. A 63 (2001) 020302(R)] using nuclear magnetic resonance quantum information processor and have experimentally verified that the payoff of the quantum game for various levels of corruption matches the theoretical payoff.

Keywords: Quantum information processing; Quantum game; Liquid state NMR

1. Introduction

Games have been studied primarily in the context of information theory. During the course of the game, the players exchange information with the other players and the referee. This immediately brings our attention to how the game will behave if the information exchanged is quantum in nature. Quantum games have been shown to have an advantage over their classical counter parts in terms of either a unique Nash Equilibrium [1,2] or a higher payoff for the optimal strategy [3,4]. Johnson [5] and Özdemir et. al. [6] had theoretically conjectured that the quantum advantage reduces if the games qubit source is corrupted by a noisy 'Demon' and above a critical value of the corruption, the quantum payoff becomes lower than the classical payoff. As noise is inherent in all forms of physical systems, studying such games in presence of corruption becomes important. While these ideas have been theoretically established, their experimental verification validates them.

Experimental implementation of a 'quantum algorithm' is still a challenging task and much research is going on in this field. Nuclear magnetic resonance (NMR) has been established as a suitable method for implementation of algorithms involving small number of qubits [9–11]. It has been used successfully to implement several quantum algorithms [12–20]. Two qubit quantum games have been implemented experimentally in NMR by Du et. al. [21] and in optical systems by Li et. al. [3]. In the present article we report the implementation of a three qubit 'Dilemma' game, with corruption in the source qubit, using NMR. To the best of our knowledge, this is the first NMR implementation of this game.

* Corresponding author. Fax: +91 80 2360 1550.
E-mail address: anilnmr@physics.iisc.ernet.in (A. Kumar).

1090-7807/$ - see front matter © 2007 Elsevier Inc. All rights reserved.
doi:10.1016/j.jmr.2007.05.013

2. The three player 'Dilemma' game

Based on the conjecture that a 'coherent quantum equilibrium' arise in a quantum game only when it involves $N \geqslant 3$ players, the three player 'Dilemma' game was created as an extension to the two player Prisoner's Dilemma game [4]. In this game the players are given a binary choice (0 or 1 which represents 'cooperate' or 'defect', respectively) and they are supposed to take independent decisions. The payoff gives us the individual gain based on the choices made by the players. Analogous to the 'el-farol' bar problem [22,23] (to which this game bears a resemblance) a set of three players have to decide whether to go to a bar or not with a sitting capacity of two. Each of the player has a deep desire to go, but does not want the bar to be over crowded or partially empty. Benjamin and Hayden found that the quantum version of the 'Dilemma' game [4] has a superior payoff as compared to its classical counterpart.

Following Johnson [5], each player is represented by a qubit and their qubits are made to pass through an three qubit entangling gate ($\mathcal{J}$). The entangling gate (Fig. 1) represented by,

$$\mathcal{J} = \frac{1}{\sqrt{2}}\left(\mathbb{I}^{\otimes 3} + i \times \sigma_x^{\otimes 3}\right), \tag{1}$$

such that

$$\mathcal{J}|000\rangle = \frac{1}{\sqrt{2}}(|000\rangle + i|111\rangle), \tag{2}$$

introduces quantum correlation between the players as shown in Eq. 2. The decision of each player, whether or not to go to the bar is represented by the unitary operators σ_x and $\mathbb{I}$ which implies 'to go' and 'not to go', respectively. After the players take their decision and play their moves, the output state is made to pass through a disentangling gate $\mathcal{J}^\dagger$ which is just a conjugate-transpose of the $\mathcal{J}$-gate, $\mathcal{J}^\dagger = \frac{1}{\sqrt{2}}(\mathbb{I}^{\otimes 3} - i \times \sigma_x^{\otimes 3})$. The final state is measured and the outcome determines the payoff of each player Table 1 [5]. If

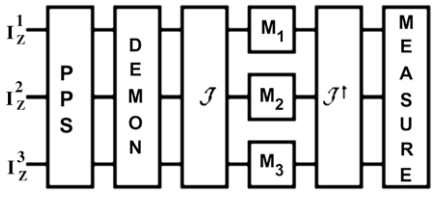

Fig. 1. The block diagram illustrating the steps of the NMR implementation of the game. In NMR, the initial state is a highly mixed state $\gamma_H I_z^H + \gamma_F I_z^F + \gamma_C I_z^C$. The pulse sequence for the creation of the PPS is applied on this state. After the creation of the PPS, pulse sequence implementing the 'Demon' is applied. This transforms the PPS to a mixed state $(1-x)|000\rangle\langle 000| + x|111\rangle\langle 111|$. Here the mixed state represents the corruption in the input (ideally the input qubits should have been in the PPS $|000\rangle$). The entangling gate (J gate) is applied after the 'Demon' after which the moves are played. Then the disentangling gate is applied and the output state is measured. Depending on the output state the payoff of the players are calculated.

Table 1
Payoff table for each player in 'Dilemma' game

Final state	Payoff
$\|000\rangle$	(0,0,0)
$\|001\rangle$	(−9,−9,1)
$\|010\rangle$	(−9,1,−9)
$\|011\rangle$	(1,9,9)
$\|100\rangle$	(1,−9,−9)
$\|101\rangle$	(9,1,9)
$\|110\rangle$	(9,9,1)
$\|111\rangle$	(2,2,2)

The left column is the final state after the game and the right column is the corresponding payoff for each player.

the final state is $|000\rangle$, it implies that all of the players have chosen 'not to go'. In this case no one gains but at the same time they are also not annoyed that somebody else has. So each of their payoff is 0. For the state $|001\rangle$, $|010\rangle$ and $|100\rangle$, only one of the players go to the bar. In this case, the player who goes to the bar is happy as he finds plenty of room there, but he has no company as the other seat is vacant. Therefore his payoff is 1. The other players are annoyed because one of them could have gone and occupied the empty seat. Therefore their payoffs are −9 each. The third possibility are the states $|011\rangle$, $|101\rangle$ and $|110\rangle$. Here, two of them goes to the bar and each of them have a seat and company. So their payoffs are 9 each. The third player is relieved that he did not give a try or else the bar would have been over crowded. Therefore his payoff is 1. The final case is the state $|111\rangle$. In this case all of them decide to go. They have a lot of company but are short of seating space. Therefore each of them has a payoff of 2 [5].

The strategy space of each of the players in the quantum version of the game consists of three choices, 'to go', 'not to go' and 'to go with a probability of half'. The choice of going to the bar corresponds to flipping the input state by applying the operator σ_x. The choice of not going to the bar corresponds to leaving the input qubit as it is by applying the identity operator and the third choice of going to the bar with a probability half corresponds to applying an operator $1/\sqrt{2}(\sigma_x + \sigma_z)$ [refer [5] and references therein for a detailed description of the discretisation of the strategy space]. Since each player has 3 choices, there are 27 possible 'configurations' of the game. Johnson has grouped these configurations into 10 different classes [5,24], with respective payoff of each class (Table 2). Starting with the input state of $|000\rangle$, the class of strategy yielding the highest payoff are (VII) and (VIII). However, class (VII) is not the Nash Equilibrium because it is not fair to all the players. So class (VIII) is the optimal strategy in this game [5]. It should be noted that the payoff of the optimal move in the quantum game is much higher than the corresponding strategy in the classical game [5]. Table 2 also contains experimental results which will be discussed in Section 4.

If the input source is corrupt, the scenario in the quantum case changes drastically. The corruption is introduced by taking the input state as $x|000\rangle\langle 000| + (1-x)|111\rangle\langle 111|$, where $x \in [0,1]$. For input $|111\rangle$ the payoff is dramatically

Table 2
The theoretical and experimental average payoff per player for ten classes of strategies

Class	$p=0$	$p=1/2$	$p=1$	Payoff, input $=\|000\rangle$		Payoff, input $=\|111\rangle$	
				Theo.	Exp.	Theo.	Exp.
I		***		−15/4	−3.65	19/4	4.33
II	*	**		−15/4	−3.44	19/4	3.88
III	**	*		−11/6	−1.59	19/6	2.81
IV	***			2	1.26	0	0.34
V			***	0	0.44	2	1.35
VI	*		**	−17/3	−5.39	19/3	5.14
VII	**		*	19/3	5.92	−17/3	−4.76
VIII	*	*	*	19/3	6.34	−17/3	−5.04
IX		**	*	19/4	4.83	−15/4	−3.10
X		*	**	−11/6	−1.87	19/6	1.65

The stars under a move indicates the number of player that have chosen that particular move. The experimental results have been calculated from the results contained in Fig. 4.

different from that of $|000\rangle$ input (see Table 2). For the optimal move, the payoff for input $|000\rangle$ is 19/3 while that for input $|111\rangle$ is −17/3. For the classical game, the corresponding payoffs are 2 and 0, respectively [5]. Thus we see that even though the quantum game offers a higher payoff of the optimal move, it deteriorates rapidly if the source is corrupt and there exists a critical value of corruption beyond which, the payoff for the optimal move in the quantum game is less than that in the classical game. It should be noted that as the players are not aware of the noise in the source qubits, they persist with their original strategy that maximize their gain for $|000\rangle$ input.

3. NMR implementation

The NMR implementation of the quantum 'Dilemma' game experimentally evaluates the effect of corruption in the input state, on the payoff of each player. The NMR implementation starts with (i) preparation of the pseudo-pure state followed by (ii) a 'Demon' which introduces a corruption of the qubits. The next step is an (iii) entanglement gate followed by (iv) moves and (v) disentangling gate. Finally the measurement yields the result.

The experiment has been carried out at room temperature in 11.7 T field in a Bruker AV500 spectrometer using a triple resonance QXI probe. The system chosen for the implementation of the game is Carbon-13 labeled $^{13}CHFBr_2$, where ^1H, ^{19}F and ^{13}C act as the three qubits. The ^1H, ^{19}F and ^{13}C resonance frequencies at this field are 500, 470 and 125 MHz, respectively. The scalar couplings between the spins are: $J_{HC}=224.5$ Hz, $J_{HF}=49.7$ Hz and $J_{FC}=-310.9$ Hz [19]. The equilibrium spectrum of each spin is given in Fig. 2a. The transition frequencies for ith spin are given by $\pm(J_{ij}\pm J_{ik})/2$ from the centre of resonance of each spin.

The NMR Hamiltonian for a three qubit weakly coupled spin system is,

$$\mathcal{H}=\sum_{i=1}^{3}\nu_i I_z^i+\sum_{i<j=1}^{3}J_{ij}I_z^iI_z^j, \tag{3}$$

where ν_i are the Larmour frequencies and the J_{ij} are the scalar couplings. The starting point of any algorithm in an NMR quantum information processor is the equilibrium density matrix, which under high temperature and high field approximation is in a highly mixed state represented by [25],

$$\begin{aligned}\rho_{eq}&=\gamma_H I_z^H+\gamma_F I_z^F+\gamma_C I_z^C\\&=\gamma_H\left(I_z^H+0.94I_z^F+0.25I_z^C\right),\end{aligned} \tag{4}$$

where the $\gamma_H{:}\gamma_F{:}\gamma_C$ is 1:0.94:0.25 are the gyromagnetic ratio of the nuclei.

The six steps for the implementation of the 'Dilemma' game with corruption in the source qubit in this three qubit system are as follows.

Step (i) Pseudo-pure state:
In a pseudo-pure state, one of the energy levels has extra or deficit population against a uniform background [26]. Since the background population, represented by a unit matrix, does not transform under a unitary transformation, the pseudo-pure state (PPS) mimics a pure state [9,10]. Here we use the method of spatial averaging [11] for the preparation of PPS. A 57.9° pulse ($\cos(57.9)=0.47$) on fluorine (qubit 2) followed by a crusher gradient transforms ρ_{eq} of Eq. (4) to $\gamma_H(I_z^H+\frac{1}{2}I_z^F+\frac{1}{4}I_z^C)$. The rest of the pulse sequence (Fig. 3a) consists of the basic sequences represented by unitary blocks $U_{i,j}^{\pi/4}$ for each J_{ij} :

$$U_{i,j}^{\pi/4}=\left[\frac{\pi}{4}\right]_{\phi}^{j}\rightarrow\frac{1}{2J_{ij}}\rightarrow\left[\frac{\pi}{4}\right]_{\phi-90}^{j}\rightarrow G_z, \tag{5}$$

where $(\alpha)_{\phi}^{j}$ represents a α degree pulse of phase ϕ on the spin j and $1/2J_{ij}$ represents the evolution time that corresponds to π rotation of the j magnetization by the coupling J_{ij}. Additional π-pulses during the free evolution period refocus the chemical shift and other J-evolutions, thus making the system evolve only under the desired J coupling[25]. G_z is the crusher gradient which removes all the transverse terms and retains only the longitudinal terms. The operator $U_{i,j}^{\pi/4}$ when applied on equilibrium density matrix $I_z^i+I_z^j$ creates $I_z^i+\frac{1}{2}(I_z^j+2I_z^iI_z^j)$. Therefore by

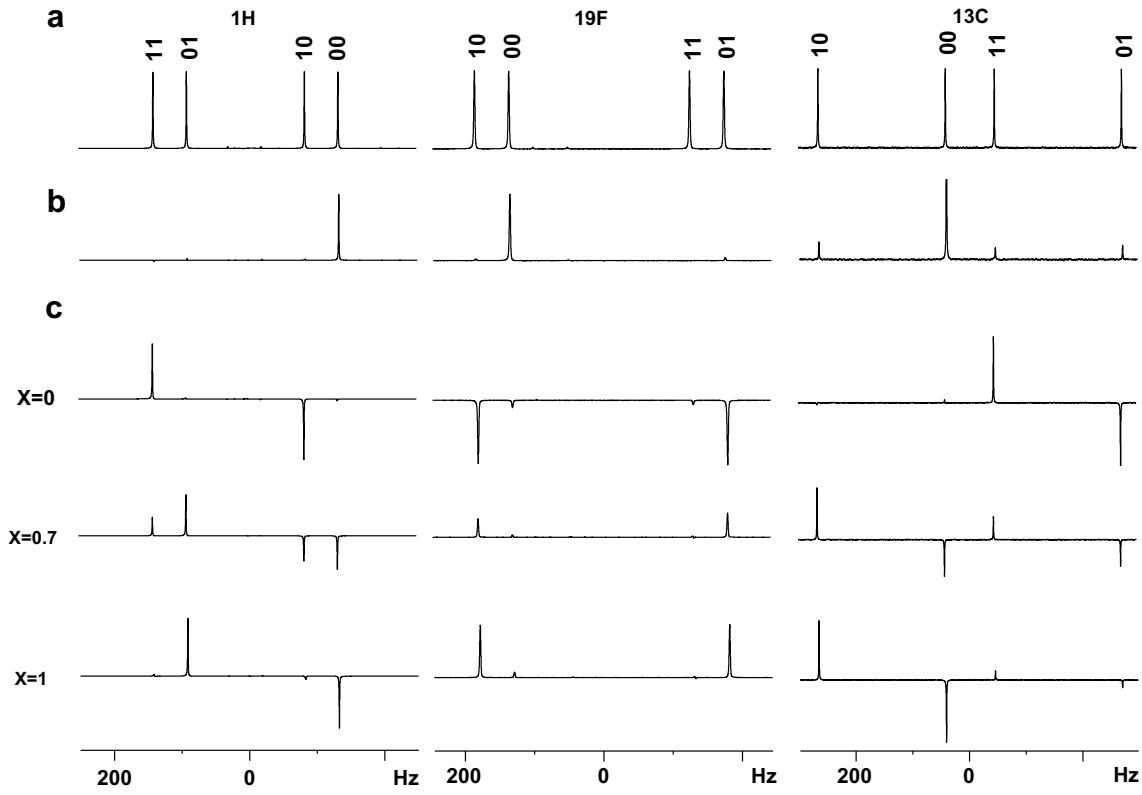

Fig. 2. (a). The equilibrium spectra of ^{1}H, ^{19}F and ^{13}C of $^{13}CHFBr_2$. The label on the top of each transition of a qubit represents the state of the other qubits in the transition. This assignment was arrived by selective inversion experiments [25]. The sample was synthesized by following the procedure given by Vendersypen [27]. 500 mg of 13C labeled bromoform ($^{13}CHBr_3$) was added to 670 mg of mercuric fluoride (HgF_2) and the mixture was refluxed gradually from 70 to 85 °C in increment of 5° for 15 min each. The reaction mixture was directly dissolved in acetone-d_6 and a bulb to bulb distillation was carried out in a 'Kugelrohr' at 65 °C. The distillation process eliminated excess of bromoform from the product to get a sample of high purity. (b) The 'population spectra' of ^{1}H, ^{19}F and ^{13}C after preparation of the pseudo-pure state. It is seen that only the transition corresponding to $|000\rangle \rightarrow |001\rangle$, $|000\rangle \rightarrow |010\rangle$ and $|000\rangle \rightarrow |100\rangle$ are present in the spectrum of PPS. This confirms, the creation of pseudo-pure state $|000\rangle$. (c) The population spectra for the optimal move (VIII). $x = 0$ implies that there is no corruption in the input state, while $x = 1$ implies that the input state is totally corrupted. $x = 0.7$ corresponds to an intermediate value of corruption. The intensity of various transition depends on the amount of corruption in each case.

applying $U_{ij}^{\pi/4}$ in the order $U_{\mathrm{HC}}^{\pi/4}, U_{\mathrm{FC}}^{\pi/4}$ and $U_{\mathrm{HF}}^{\pi/4}$ on the density matrix $I_z^{\mathrm{H}} + \frac{1}{2}I_z^{\mathrm{F}} + \frac{1}{4}I_z^{\mathrm{C}}$ yields,

$$\rho_{\mathrm{pps}} = \frac{\gamma_{\mathrm{H}}}{4}\left(I_z^{\mathrm{H}} + I_z^{\mathrm{F}} + I_z^{\mathrm{C}} + 2I_z^{\mathrm{H}}I_z^{\mathrm{F}} + 2I_z^{\mathrm{H}}I_z^{\mathrm{C}} + 2I_z^{\mathrm{F}}I_z^{\mathrm{C}} + 4I_z^{\mathrm{H}}I_z^{\mathrm{F}}I_z^{\mathrm{C}}\right), \tag{6}$$

which is the spin operator representation for the $|000\rangle$ PPS [26]. The experimental spectra obtained after the preparation of the $|000\rangle$ PPS are given in Fig. 2b. The experimental spectra confirm the preparation of $|000\rangle$ PPS.

Step (ii) 'Demon':

The second step is the application of the 'Demon'. The 'Demon' creates a mixture of state $|000\rangle$ and $|111\rangle$. A Θ degree pulse on protons transforms $|000\rangle$ to $\sqrt{(1-x)}|000\rangle + \sqrt{x}|100\rangle$. After the Θ degree pulse (Fig. 3b) the system is evolved under J_{HC} for a time period of $1/2J_{\mathrm{HC}}$ followed by J_{FC} for a time period of $1/2J_{\mathrm{FC}}$. At the end a crusher gradient is applied to remove all the transverse magnetization. This transforms the above state to

$$\rho_{\mathrm{Demon}} = (1-x)|000\rangle\langle 000| + x|111\rangle\langle 111|, \quad x \in [0,1], \tag{7}$$

where x is $\sin^2(\Theta/2)$. For $\Theta = 0$, x is 0 and we have only $|000\rangle$ state, for $\Theta = 180$, $x = 1$, we have only $|111\rangle$ state and for any intermediate value of Θ we have a mixed state given by Eq. (7).

Step (iii) Entangling $\mathcal{J}$-gate:

Following the 'Demon' we apply an entangling $\mathcal{J}$-gate and the pulse sequence for its implementation is given in Fig. 3(c). The $\mathcal{J}$-gate involves the implementation of $\mathbb{I}^{\otimes 3} + i \times \sigma_x^{\otimes 3}$ operator. The $\mathcal{J}$-gate sequence consists of three J-evolution sandwiched between 90° pulses. To implement the $\mathcal{J}$-gate the system has to be evolved under a unitary operator of the form $\exp(-i\pi I_x^{\mathrm{H}} I_x^{\mathrm{F}} I_x^{\mathrm{C}})$. The pulse sequence given in Fig. 3(c) achieves this in the following manner: the system is evolved under the unitary operator $U_{\mathrm{FC}}^{\pi/2}$, which consists of evolution under the J_{FC} for a period $\tau = 1/2J_{\mathrm{FC}}$ sandwiched between two $\pi/2$ pulses of given phases on carbon, yielding

$$\begin{aligned} U_{\mathrm{FC}}^{\pi/2} &= \left[\exp\left(-i\left[\frac{\pi}{2}\right]I_x^{\mathrm{C}}\right)\right] \cdot \left[\exp\left(-i2\pi J_{\mathrm{FC}} I_z^{\mathrm{F}} I_z^{\mathrm{C}} \tau\right)\right] \cdot \left[\exp\left(i\left[\frac{\pi}{2}\right]I_x^{\mathrm{F}}\right)\right] \\ &= \exp\left(-i\pi I_z^{\mathrm{F}} I_y^{\mathrm{C}}\right). \end{aligned} \tag{8}$$

Similarly the evolutions under $U_{\mathrm{HC}}^{\pi/2}$ is achieved by evolving under the J_{HC} for a period $\tau = 1/2J_{\mathrm{HC}}$, juxtaposed between two $\pi/2$ pulses on proton yielding,

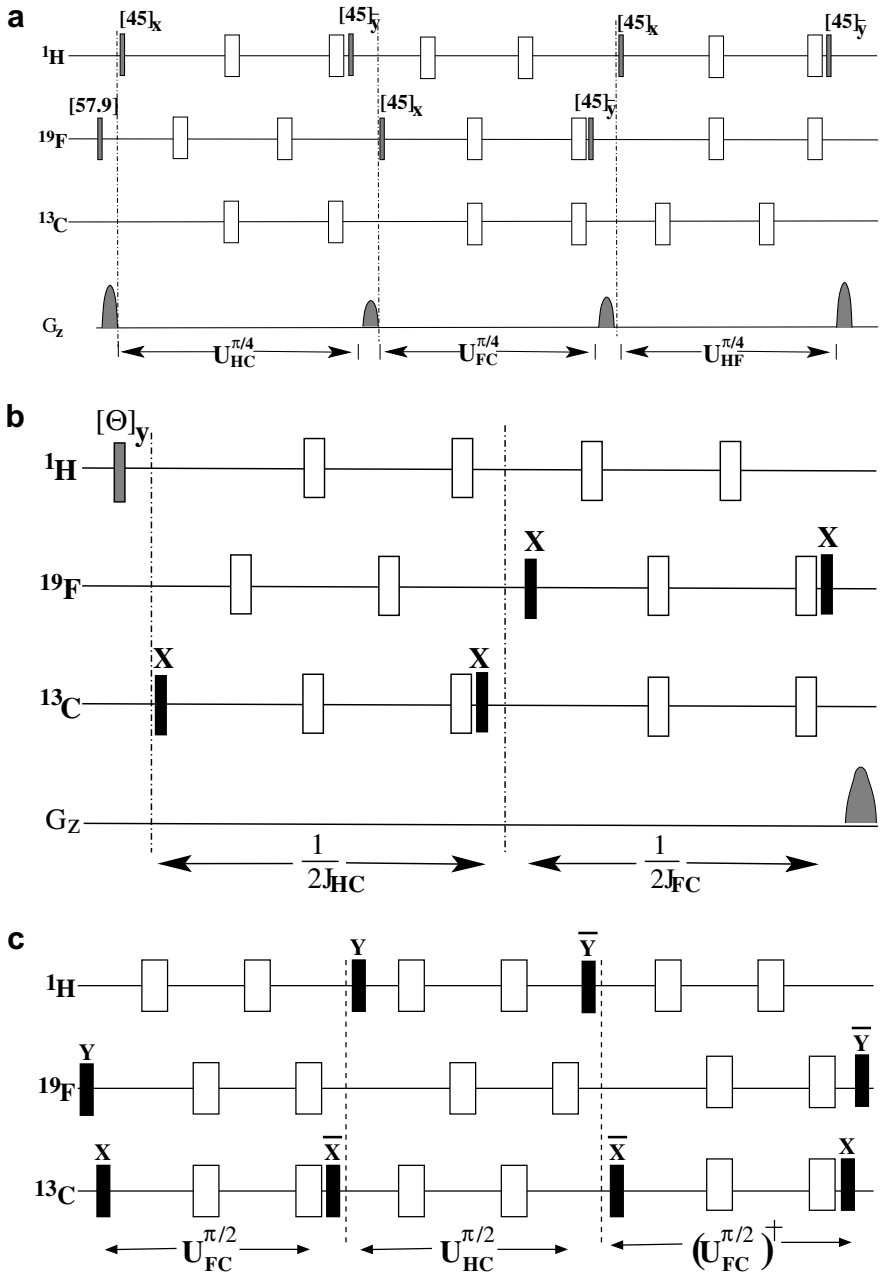

Fig. 3. The pulse sequence for the implementation of the (a) PPS, (b) 'Demon' and the (c) $\mathcal{J}$-gate. The broad white pulses are 180° and the narrow black pulses are 90°. The flip angle of the other pulses as well as the relevant phases of all the pulses are also written above them. The series of pulses along the G_z line implies z gradient. The period of $1/2J_{\alpha\beta}$, where α, β are H of F or C, implies evolution only under the scalar coupling Hamiltonian, $2\pi J_{\alpha\beta} I_z^{\alpha} I_z^{\beta}$ for that time period. Evolutions under all other couplings as well as the chemical shift evolutions have been refocused during this period.

$$U_{\mathrm{HC}}^{\pi/2} = \left[\exp\left(-i\left[\frac{\pi}{2}\right]I_y^{\mathrm{H}}\right)\right]\cdot\left[\exp\left(-i2\pi J_{\mathrm{HC}} I_z^{\mathrm{H}} I_z^{\mathrm{C}}\tau\right)\right]\cdot\left[\exp\left(i\left[\frac{\pi}{2}\right]I_y^{\mathrm{H}}\right)\right] = \exp\left(-i\pi I_x^{\mathrm{H}} I_z^{\mathrm{C}}\right). \quad (9)$$

On applying $U_{\mathrm{FC}}^{\pi/2} - U_{\mathrm{HC}}^{\pi/2} - (U_{\mathrm{FC}}^{\pi/2})^{\dagger}$, in sequence, the effective evolution is,

$$\left[\exp\left(-i\pi I_z^{\mathrm{F}} I_y^{\mathrm{C}}\right)\right]\cdot\left[\exp\left(-i\pi I_x^{\mathrm{H}} I_z^{\mathrm{C}}\right)\right]\cdot\left[\exp\left(-i\pi I_z^{\mathrm{F}} I_y^{\mathrm{C}}\right)\right] = \exp\left(-i\pi I_x^{\mathrm{H}} I_z^{\mathrm{F}} I_x^{\mathrm{C}}\right). \quad (10)$$

Finally, on applying the $\pi/2$ pulses on the fluorine spin at the beginning and end of the above evolution of Eq. (10), the system is effectively evolved under the unitary operator,

$$\left[\exp\left(-i\left[\frac{\pi}{2}\right]I_y^{\mathrm{F}}\right)\right]\cdot\left[\exp\left(-i\pi I_x^{\mathrm{H}} I_z^{\mathrm{F}} I_x^{\mathrm{C}}\right)\right]\cdot\left[\exp\left(i\left[\frac{\pi}{2}\right]I_y^{\mathrm{F}}\right)\right] = \exp\left(-i\pi I_x^{\mathrm{H}} I_x^{\mathrm{F}} I_x^{\mathrm{C}}\right) \quad (11)$$

Thus the unitary operator of Eq. (11), implements the entangling $\mathcal{J}$-gate.

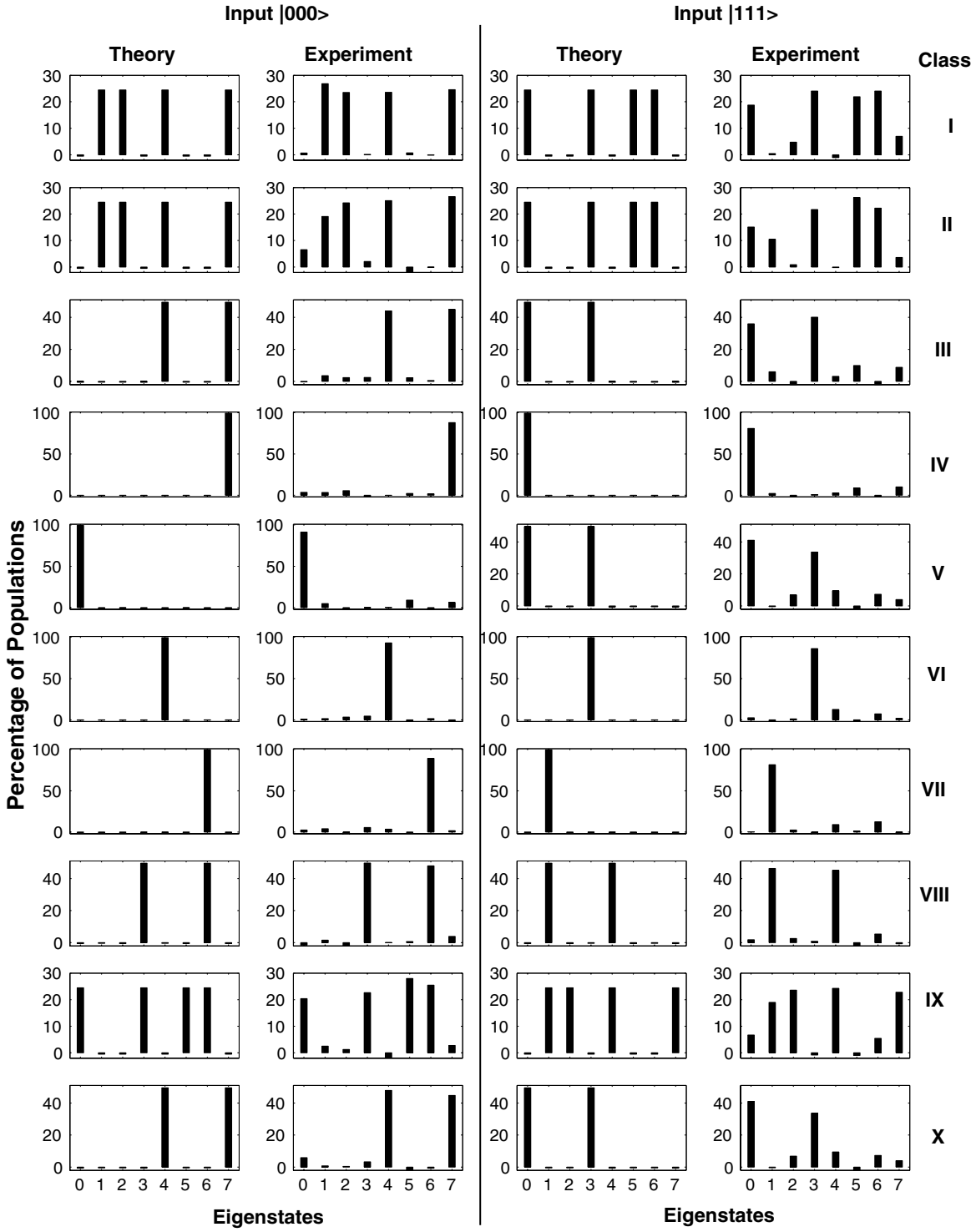

Fig. 4. Theoretical and experimental bar plot of the diagonal elements of the final density matrix for inputs $|000\rangle$ and $|111\rangle$ for all classes of moves. The numbers 0 to 7 in the horizontal axis of each bar plot represent the states $|000\rangle$, $|001\rangle$, $|010\rangle$, $|011\rangle$, $|100\rangle$, $|101\rangle$, $|110\rangle$ and $|111\rangle$, respectively. The vertical axis of each bar plot is in percentage of populations. Therefore the height of the bars depict the population of each diagonal term of the density matrix in percentage.

Step (iv) Moves:

After the entangling gate, the players play their moves (Table 2). The moves are (a) 'do not flip one's state' that corresponds to $p = 1$, (b) 'flip state' that corresponds to $p = 0$ and (c) 'flip state with a probability half' that corresponds to $p = \frac{1}{2}$ in the Table 2. The move 'do not flip' implies that the player does not do anything with his qubit. So this is equivalent to no operation. The move 'flip state' implies that the player flips the state of his qubit. This is equivalent to σ_x which corresponds to a $[\pi]_x$ pulse in

NMR. The move 'flip state with a probability half' corresponds to the operator $\frac{1}{\sqrt{2}}(\sigma_z + \sigma_x)$ which can be implemented by a $[\frac{\pi}{2}]_x$ pulse, on the desired spin.

Step (v) Disentangling $\mathcal{J}$-gate:

After application of the moves according to the requirements in various cases for the game, the $\mathcal{J}^\dagger$-gate is applied. The $\mathcal{J}^\dagger$-gate is the conjugate-transpose of the $\mathcal{J}$-gate and is applied in NMR by changing the phase of all the $\pi/2$ pulses in Fig. 3(c) by π.

Step (vi) Measurement:

The final information is coded in the diagonal elements of the density matrix (population of various eigenstates). These are measured by using 90° measuring pulses on each spin yielding ''population spectra''. Prior to application of the 90° measuring pulses, a crusher gradient G_z is applied to destroy any undesirable coherences created by the preceding operations. To calculate the payoff for each player, the diagonal elements of the density matrix are multiplied by the payoff of the individual player for each outcome. The equation for the payoff of the ith player is given by [5]

$$\$_i = \sum_{abc} \$_i^{abc} P_{abc} \quad \text{where} \quad a, b, c \in \{0, 1\}. \tag{12}$$

Here $\$_i$ is the payoff of the ith player, $\$_i^{abc}$ is the payoff of the ith player corresponding to the output $|abc\rangle\langle abc|$ and P_{abc} is the probability with which the state $|abc\rangle\langle abc|$ occurs. Finally the average payoff per person is calculated by

$$\langle \$ \rangle = \frac{1}{3} \sum_{i=1}^{3} \$_i. \tag{13}$$

4. Results and conclusion

The simulated and the experimental diagonal elements of the density matrix for the input $|000\rangle$ and $|111\rangle$ for various classes of Table 2 are given in Fig. 4. The experimental populations reproduce the expected theoretical populations with an average error of ~15% when the input is $|000\rangle$ and an average error of ~20% when the input is $|111\rangle$. The errors are mainly due to r.f. inhomogeneity (verified by simulation).

For the optimal case (case VIII), the experiments were performed with corruption by using various values of Θ degree pulse on proton followed by the evolution under J_{HC} and J_{FC} to reach the state given by Eq. (7). 'x' was varied in 11 steps and the results of three of them (for $x = 0$, 0.7 and 1) are plotted in Fig. 2c. For $x = 0$, the input state is $|000\rangle$ and the output state has populations only in states 3 ($\equiv|011\rangle$) and state 6 ($\equiv|110\rangle$) (Fig. 4). The spectra in Fig. 2c for $x = 0$, having two positive and four negative lines at the right frequencies, confirms this result. Similarly for $x = 1$, the input state is $|111\rangle$ and the output state has populations only in states 1 ($\equiv|001\rangle$) and 4 ($\equiv|100\rangle$) (Fig. 4). The spectrum of Fig. 2c for $x = 1$ also confirms this result. For the

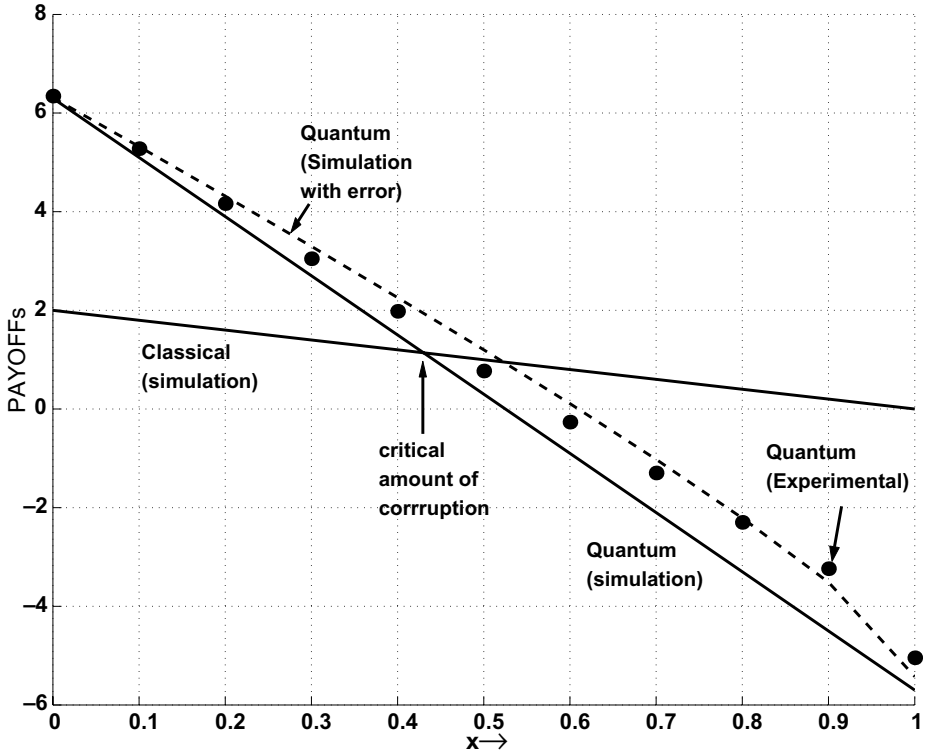

Fig. 5. The plot of simulated classical and quantum (continuous lines) and experimental (dots) 'average payoff per person' vs 'the amount of corruption' for the quantum game. The experimental payoff matches the expected payoff for all values of corruption. However, the expected payoff $x > 0.5$ has not decreased to expected result mainly due to r.f. inhomogeneities in the Θ degree pulse. A simulation of the expected result for a 10% error in Θ degree pulse is shown by the dashed line (- - -), which matches the experimental result.

intermediate value of $x = 0.7$, these states are populated to various degrees and the result is given in Fig. 2c. From these spectra the average payoff is calculated using Eq. (13) and the results are plotted in Fig. 5 for all the 11 experiments. Fig. 5 also contains a simulation of expected results for quantum and classical version of the game as a function of the corruption x. The experimental results validate the expected quantum results for all levels of corruption. The experimental payoff crosses over below the classical limit around the expected critical corruption.

We have thus implemented the quantum 'Dilemma' game of Johnson [5] using a three qubit NMR system and verified the quantum payoff for all levels of corruption. Quantum games have important application in communication theory and market strategies. We hope that this work leads to more experimental verification of other quantum games. One of the possible extension of this problem would be to implement the evolutionary version of the game [28].

Acknowledgments

We would like to thank Prof. S. Chandrasekaran of Department of Organic Chemistry of our Institute for the synthesis of the three qubit sample used here. We would also like to thank Mr. Ramkumar for his help during the sample preparation. The use of AV-500 NMR spectrometer funded by the Department of Science and Technology (DST), New Delhi, at the NMR Research Centre, Indian Institute of Science, Bangalore, is gratefully acknowledged. A.K. acknowledges DAE for Raja Ramanna Fellowship, and DST for a research grant on ''Quantum Computing using NMR techniques''.

References

[1] J. Eisert, M. Wilkins, M. Lewenstein, Phys. Rev. Lett. 83 (1999) 3077.
[2] L. Marinatto, T. Weber, Phys. Lett. A 272 (2000) 291.
[3] H. Li, J. Du, S. Massar, Phys. Lett. A 306 (2002) 73.
[4] S.C. Benjamin, P.M. Hayden, Phys. Rev. A 64 (2001), 030301(R).
[5] N.F. Johnson, Phys. Rev. A 63 (2001), 020302(R).
[6] S.K. Ozdemir, J. Shimamura, N. Imoto, quant-ph/0402038.
[9] D.G. Cory, A.F. Fahmy, T.F. Havel, Proc. Natl. Acad. Sci. USA 94 (1997) 1634.
[10] N. Gershenfeld, I.L. Chuang, Science 275 (1997) 350.
[11] D.G. Cory, M.D. Price, T.F. Havel, Physica D 120 (1998) 82.
[12] I.L. Chuang, L.M.K. Vanderspyen, X. Zhou, D.W. Leung, S. Llyod, Nature 393 (1998) 143.
[13] J.A. Jones, M. Mosca, J. Chem. Phys. 109 (1998) 1648.
[14] Kavita Dorai, Arvind, Anil Kumar, Phys. Rev. A. 61 (2000) 042306.
[15] Ranabir Das, Anil Kumar, Phys. Rev. A. 68 (2003) 032304.
[16] I.L. Chuang, N. Gershenfeld, M. Kubinec, Phys. Rev. Lett. 80 (1998) 3408.
[17] J.A. Jones, M. Mosca, R.H. Hansen, Nature 393 (1998) 344.
[18] L.M.K. Vanderspyen, Matthias Steffen, Gregory Breyta, C.S. Yannoni, M.H. Sherwood, I.L. Chuang, Nature 414 (2001) 883.
[19] M. Steffen, W. van Dam, T. Hogg, G. Bryeta, I. Chuang, Phys. Rev. Lett. 90 (2003) 067903.
[20] Avik Mitra, Arindam Ghosh, Ranabir Das, Apoorva Patel, Anil Kumar, J. Magn. Res. 177 (2005) 285–298.
[21] Jiangfeng Du, Hui Li, Xiaodong Xu, Mingjun Shi, Jihui Wu, Xianyi Zhou, Rongdian Han, Phys. Rev. Lett. 88 (2002) 137902.
[22] B.W. Arthur, Am. Econ. Assoc. 84 (1994) 406.
[23] N.F. Johnson, S. Jarvis, R. Jonson, P. Cheung, Y. Kwong, P.M. Hui, Physica A 258 (1998) 230.
[24] N.F. Johnson, P.M. Lui, R. Jonson, T.S. Lo, Phys. Rev. Lett. 82 (1999) 3360.
[25] Principles of Nuclear Magnetic Resonance in One and Two Dimensions, Oxford University Press, New York, 1994.
[26] M.A. Nielsen, I.C. Chuang, Quantum Computation and Quantum Information, Cambridge University Press, 2000.
[27] L.M.K. Vanedrsypen, Experimental Quantum Computation with Nuclear Spins in Liquid Solution, Doctoral Thesis (2001) pp. 167.
[28] R. Kay, N.F. Johnson, S.C. Benjamin, J. Phys. A: Math. Gen. 34 (2001) L547–L552.